Korean Journal of Remote Sensing, Vol.19, No.5, 2003, pp.371~380

Generation of Forest Leaf Area Index (LAI) Map Using Multispectral Satellite Data and Field Measurements

Kyu-Sung Lee, Sun-Hwa Kim, Yoon-Il Park, and Ki-Chang Jang

Inha University, Department of Geoinformatic Engineering

Abstract : The primary objective of this study is to develop a suitable methodology to generate forest leaf area index (LAI) map at regional and local scales. To build empirical models, we collected the LAI values at 30 sample plots over the forest within the Kyongan watershed area by the field measurements using an optical instrument. Landsat-7 ETM+ multispectral data obtained at the same growing season with the field LAI measurement were used. Three datasets of remote sensing signal were prepared for analyzing the relationship with the field measured LAI value and they include raw DN, atmospherically corrected reflectance, and topographically corrected reflectance. From the correlation analysis and regression model development, we found that the radiometric correction of topographic effects was very critical step to increase the sensitivity of the multispectral reflectance to LAI. In addition, the empirical model to generate forest LAI map should be separately developed for each of coniferous and deciduous forest.

Key Words : Forest LAI, Radiometric Correction, Vegetation Index, ETM+.

1. Introduction

Leaf area index (LAI) has been one of the most useful and important parameters in quantitative aspects of vegetative remote sensing. LAI, defined as the sum of the leaf area per unit ground area, can be used to estimate photosynthesis, evapotranspiration, and the productivity of plant ecosystem (Bonan, 1993). The measurement of LAI on the ground is very difficult and requires a great amount of time and efforts (Gower *et al.*, 1999). It is particularly true to measure LAI in forest where the vegetation structure is much more complex than any other biomes. Since forest canopy is mainly composed of leaves, which is the direct source of solar radiation reflected to earth-observing remote sensing systems, LAI has been an attractive variable of interest in terrestrial remote sensing.

There have been numerous attempts to estimate LAI using satellite remote sensor data since the early stage of space remote sensing (Badhwar *et al.*, 1986; Turner *et al.*, 1999). Remote sensing estimation of LAI has been primarily based upon the empirical relationship between the field measured LAI and sensor observed spectral responses or to spectral vegetation indices (Curran *et al.*, 1992). To produce an LAI map of a large geographic area, regression modeling to relate field data with

Received 8 September 2003; Accepted 5 October 2003.

remote sensing data has been a typical methodology. Several spectral vegetation indices (VI) and spectral reflectance have been applied for LAI estimation, in which the normalized difference vegetation index (NDVI) using near infrared band and red band was the most commonly used. However, NDVI showed the saturation phenomenon, which is not very sensitive at high LAI value (Chen and Cihlar, 1996; Carlson and Reley, 1997; Eklundh *et al.*, 2001).

Although empirical models are important tool for relating field-measured biophysical variables to remote sensing data, several factors have certain influences on the empirical relationships (Cohen *et al.*, 2003). In empirical modeling of estimating LAI over large geographic area, both field measurement of LAI and spectral reflectance obtained from satellite image data are not error-free and varies by several steps of data collection procedure. Forest type, canopy structure, background (soil and litter), and modeling methodology are among those factors that affects the empirical modeling (Panferov *et al.*, 2001; Tian *et al.*, 2000; Fassnacht and Stith, 1997). In addition, the sensor-received signals can also vary by the atmospheric condition at the time of data acquisition and the solar illumination effects of topographic slope and aspects.

In this study, we are attempting to define a methodology to generate LAI map by empirical modeling to link the field measured LAI and satellite multispectral data. Although forest occupies two third of total land and plays an important role to sustain healthy environmental condition in Korea, it is very rare to find any studies related to the LAI estimation/measurement in forest. The objectives of this study are to develop appropriate procedures for measuring forest LAI on the ground and to evaluate the effects of preprocessing of satellite multispectral image data to build the optimum empirical model for generating LAI map, in particular for the forest in Korea.

2. Field LAI Measurements

1) Study Area

The study was conducted at the Kyongan Watershed located in southeast of the Seoul metropolitan area in central Korea. The Kyongan River is a subsidiary branch of the Han River. The study area includes a total size of 561km^2 and 67% of them is covered by forest lands. One third of the forest is coniferous plantation stands of Korean pine (*Pinus koraiensis*), Pitch pine (*Pinus rigida*), and Larch (*Larix leptolepis*). The remaining two third of the forests is natural forest of mixed deciduous species, in which the dominant species are oaks (*Quercus mongolica*) mixed with natural pine species. Except for a few plantation forests, most forests have very dense canopy closure over 80% and average tree age ranges from 20 to 50 years. The study area has been an experimental watershed for many years to study local-scale runoff and water quality monitoring, in which site-specific LAI estimate can be a variable of interest for the hydrological studies.

2) LAI measurements

Field measurement of LAI can be divided into two major approaches of direct and indirect method (Chen *et al.*, 1999; Gower *et al.*, 1999). Direct method essentially based upon the collection of all leaves within unit area and includes destructive harvest and litter-fall collection. The direct methods were primarily applied in agriculture crop and grassland area. It is difficult and time-consuming to apply such direct method in forest situation where the distribution of leaves are much more complex than the crop and grass land. A slightly modified direct method that had been used in forest is the application of allometric equation that relates total leaf area of a tree as a function of diameter at breast height (DBH) and/or tree height. The development and

use of allometric equations are, however, often limited by site-specific conditions of forest stands, which include tree species, age, stand density, and growing conditions. In recent years, several optical devices become available for the indirect measurement of LAI. The basic concept of optical LAI measurement is to invert a canopy gap fraction model that describes the amount of light penetrating tree canopy as a function of leaf area and distribution. Although Kim and Lee (2003) used one of such optical instruments to estimate LAI in temperate forest in Korea, their LAI estimates have not been quite verified and calibrated yet.

For the study, we used the Li-Cor LAI 2000 plant canopy analyzer, which is a commercial instrument to indirectly measure LAI. Like other similar optical instruments, the Li-Cor 2000 estimates LAI by measuring light transmittance under the forest canopy. To obtain LAI, it requires two measurements above and below the vegetation canopy. The above measurement is for determining the amount of light illuminating over the canopy and the below measurement is for determining the amount of light penetrating through the canopy. The canopy transmittance can be calculated by subtracting the below measurement from the above measurement. The inversion from canopy transmittance to LAI is based on the canopy gap fraction model, which assumes that canopy composed of randomly distributed leaves (Li-Cor, 1992; Stenberg *et al.*, 2003).

Using the forest stand maps showing the major tree species, age class, DBH class, and stand density, we selected 30 ground plots over the study area. The 30 ground plots were selected to include diverse forest types of both coniferous and natural stands. Field measurements were conducted during the three days from September 15 to September 17, 2003. Each plot has an area of $20 \times 20 m^2$ and includes five subplots for LAI measurements within it. LAI was measured three times at each subplot and total of 15 measurements were averaged to obtain the LAI value for each plot. The exact locations of the 30 ground plots were obtained using a differential global positioning system (GPS). Fig. 1 shows the distribution of the 30 plots within the boundary of the Kyongan River basin.

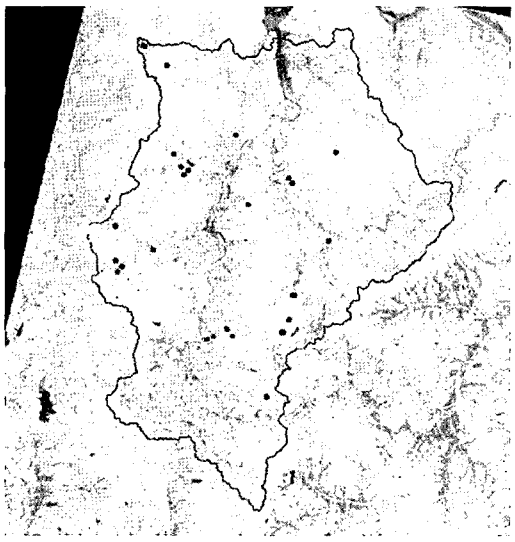

Fig. 1. Distribution of 30 ground plots for the field LAI measurements within the boundary of the Kyongan River basin covering $561 km^2$.

3. ETM+ Data Processing

Landsat-7 ETM+ multispectral data were chosen for generating LAI map. Although there are several other satellite multispectral data, we believe that Landsat data have adequate set of spatial, spectral, radiometric and temporal resolution than any other remote sensor data. To minimize any discrepancies due to the phenological variation of leaf development, the ETM+ data captured on September 10, 2002 were selected for the study. Although the ETM+ data acquisition was one year earlier than the field measurement, we believe that it did not cause any problem since the leaf development and the actual canopy condition between 2002 and 2003 were not much different. The ETM+ data were initially georeferenced to a plane rectangular coordinate system

by using a set of ground control points (GCP) obtained from the 1:5,000 scale topographic maps.

As remote sensing signal corresponding to the field measured LAI value, it would be simple and easy if we use the raw digital number (DN) value that is the most common data product provided. Although DN value represents a certain amount of radiometric quantity that was reflected from the canopy, it also includes partial signal originated by atmospheric and topographic attenuation. The empirical model to link the field measured LAI and remote sensor signal, we built two additional datasets through the radiometric correction of the raw DN value. The raw DN value was converted to percent reflectance after the atmospheric correction. Further radiometric correction was applied to reduce the topographic slope and aspect effects.

1) Atmospheric Correction

Atmospheric correction has become a critical step for deriving any quantitative variables of biophysical parameters from optical remote sensing data. However, it is rather complex and difficult to apply the absolute correction of atmospheric effects on multispectral data such as ETM+ due to the lack necessary information. The atmospheric correction requires a complete set of atmospheric data at the time of image data acquisition, which are highly variable in both spatially and temporally and often very difficult to obtain.

Once the DN value was converted to the sensor-received radiance (Lt) by applying gain and offset coefficients, the relationship between the reflectance from the target and the sensor-received radiance can be summarized as follow.

$$\rho = \frac{\pi(L_t - L_p)}{T_v(E_o \cos\theta_z T_z) + E_d} \quad (1)$$

ρ : Reflectance

L_t : Sensor-received radiance

L_p : Path Radiance

T_v : Transmittance from target to sensor

T_z : Transmittance from sun to target

E_o : Extraterrestrial solar irradiance

E_d : Diffuse sky irradiance

θ_z : Solar zenith angle

To solve for the reflectance (ρ) in above equation to, we need to know other parameters in right side of the equation. To obtain the values of L_p, T, and E_d, we used the MODTRAN radiative transfer model. Although this model requires several atmospheric data at the time of data acquisition, it is impossible to get such complete set of atmospheric data. We used a model atmosphere and a few parameters, such as atmospheric humidity, that were obtained from the local weather stations to run the model and calculated necessary parameters. Although absolute correction of atmospheric attenuation may still be an on-going efforts and very tricky job, it provides close representation of reflectance that is more directly related the biophysical characteristics of target.

2) Radiometric Correction of Topographic Effects

ETM+ reflectance data were further processed to reduce the radiometric distortion caused by topographic slope and aspects. Optical remote sensing data collected over rugged terrain reveal variable brightness values due to the different illumination angles and reflection geometry. In such cases, the pixel brightness value cannot be used as a pure representation of the reflected radiant flux from the target of interest. The study area has mountainous topography and shows distinct tonal variation due to the topographic effects. To reduce the topographic effects on the ETM+ data, we applied the radiometric correction method suggested by Smith *et al.* (1980). Minnaert's method was effective to correct the topographically induced radiometric distortions over the forests in Korea (Lee and Yoon, 1997). The sensor-received radiance is a function of normalized radiance and illumination geometry.

$$L = L_n \cos^k i \cos^{k-1} e \quad (2)$$

L : sensor-received radiance

L_n : normalized radiance

i : local incidence angle

e : slope angle

k : Minnaert constant

For each pixel location, local incidence angle i and slope angle e were obtained from the digital elevation model (DEM) data over the study area. In solving for the topographic corrected radiance L_n, only unknown parameter was Minnaert constant k. The constant k was computed empirically by converting the equation (2) into the form of simple regression function as follows.

$$\log(L\cos e) = \log L_n = k\log(\cos i \cos e) \quad (3)$$

The forest stand maps were overlaid to the geocoded ETM+ image and extract all the pixels within the boundaries of a few stands of homogeneous forest. These forest stands have identical species composition, tree size, and crown density. Considering that the forest in a polygon has rather uniform structure, the tonal variation among the pixels within a stand can be thought as the effect of topographic slope and aspect. The left-side term and the second part of right side (*cosi cose*) in equation (3) were derived from the DEM and image data within the boundary of the sample stands. The Minnaert constant k was, in fact, the slope of two known variables. Fig. 2 shows the empirically calculated k values for each spectral band of the ETM+ data used for the study.

After the Minnaert constant k was derived, the topographic correction was applied to each band of the ETM+ data. Fig. 3 compares the result of radiometric correction of topographic effects. The evident variations of brightness seen on the uncorrected images are greatly diminished after the correction by the Minnaert's method. From visual interpretation of these two images, the tonal variation on topographic slope and aspect seems to be properly normalized and both sides of slope have well balanced brightness.

3) Relating the field measured LAI and spectral Reflectance

A vector file of 30 ground plots was overlaid to each of three georectified ETM+ datasets (DN, atmospherically corrected reflectance, and topographically corrected reflectance), the pixels corresponding to each plot were extracted. Three or four

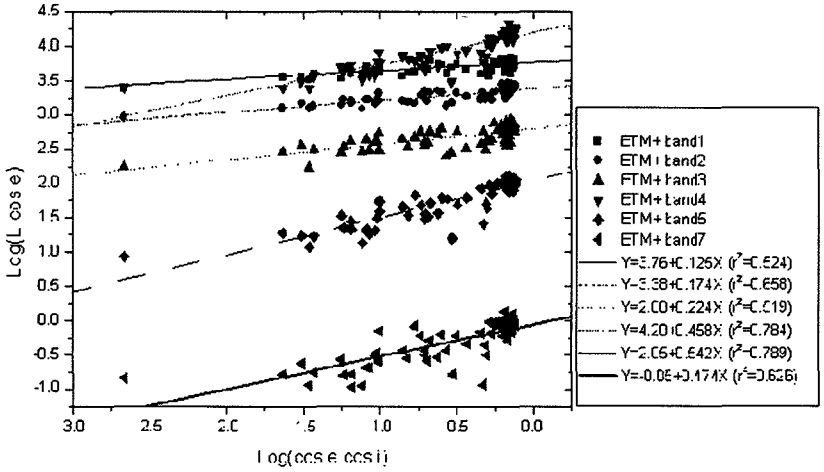

Fig. 2. Determination of the Minnaert constant k, which is a slope of regression function in equation (3), of the ETM+ data used for the study.

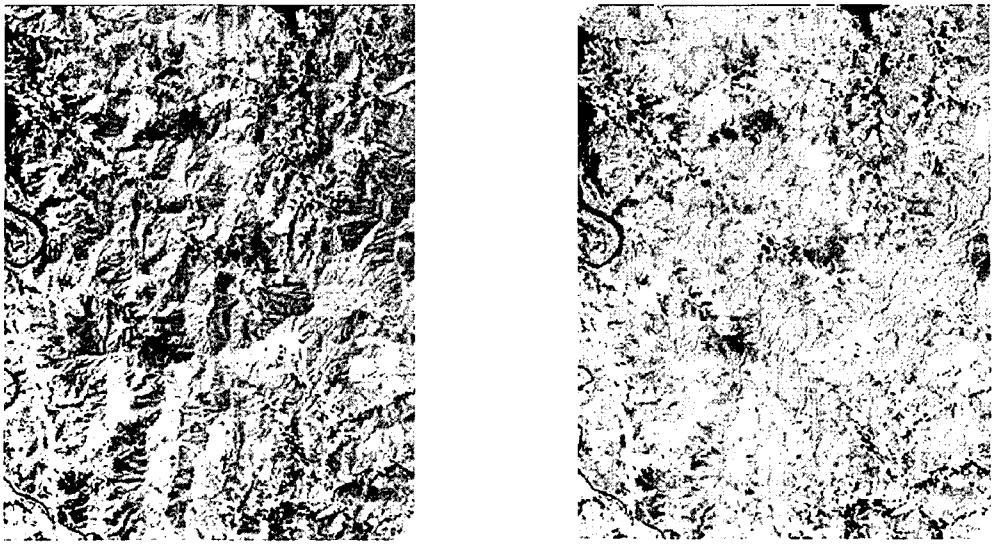

Fig. 3. Radiometric correction of topographic effects over mountainous forest in the study area. The total variation by slope and aspect on the raw image (left) is greatly diminished by the Minnaert correction (right).

pixels were spanned by the boundary of each plot of 20 meters radius. Data values of those pixels were extracted from each band and they were averaged. Due to the high spatial autocorrelation, the variation of adjacent pixels was very low to overcome the problem of the sub-pixel error distance of the geometric registration.

Initial approach to compare the field measured LAI and the ETM+ reflectance was a simple correlation analysis. The empirical models to link the spectral reflectance to the field measured LAI were developed separately for each forest type as well as for all forest types. Although the use of a single value of a spectral vegetation index (SVI), such as normalized difference vegetation index (NDVI) or simple ratio (SR), have been widely applied on modeling of empirical relationship, they utilize only a fraction of the spectral information available in several spectral bands. In this study, we tried to use several SVI's as independent variables to model the relationship with the field measured LAI. In addition to the NDVI, we also derived other SVIs that could provide the full range of spectral information of the ETM+ bands. The reduced simple ratio (RSR) was designed to use for all forest type of deciduous and coniferous species (Brown *et al.*, 2000). The RSR is a modified form of SR by introducing shortwave infrared (SWIR) reflectance. As seen in the equation (4), the RSR was calculated by reducing the SR by the difference between the SWIR reflectance and the minimum SWIR reflectance. We use the ETM+ band-5 for obtaining the SWIR reflectance.

$$RSR = \frac{NIR}{R}\left[1 - \left(\frac{SWIR - SWIR_{\min}}{SWIR_{\max} - SWIR_{\min}}\right)\right] \quad (4)$$

We also created three other indices of brightness (BR), greenness (GN), and wetness (WT) by the tasseled cap (TC) transformation (Crist, 1985). We used the transformation coefficients for the Landsat-7 ETM+ data were provided by Huang *et al.* (2002).

4. Results and Discussions

Although we selected the ground plots to include wide range of stand characteristics, the measured LAI values have relatively narrow range. The average LAI

value for all plots is 4.18 with a standard deviation of 0.88, except for one plot of very young dense pine plantation which showed very high LAI value. Since this plot is very different in tree size, density, and tree age from other stands, we decided to exclude it from further analysis. Almost every plot we visited show very dense canopy closure regardless of the tree size and species. Mean LAI value (5.60) of the plantation coniferous forest is slightly higher than the one (3.64) from the natural stands of mixed deciduous forest.

As pointed from previous studies (Gower *et al.*, 1999), the LAI measurement by the Li-2000 instrument may not necessarily provide an accurate measure of LAI. Although we used clumping factors to adjust the non-random leaf distribution of coniferous trees, they have not been completely calibrated for the forest stands in Korea. To achieve more reliable and accurate measure of LAI in the field, we need to have rather comprehensive approach to calibrate the Li-2000 LAI measurement by using the direct LAI measurement.

In overall, correlation coefficients between the spectral reflectance and the field measured LAI were relatively low for all plots combined in three dataset (Table 1). Forest LAI varies by several factors of stand structural parameters, such as species, stand density, crown closure, DBH, and tree height. Considering the diverse groups of species composition and dense canopy conditions over the study area, such low correlations would not be surprising.

When we calculated the correlation coefficient separately for each of two species groups of coniferous and mixed deciduous forest, the absolute value of correlation coefficients increased at the coniferous forest. The plantation coniferous stands are rather homogeneous in species composition. The variation of LAI in these stands is mainly due to the tree size and stand density. It is rather unusual to see the low correlations between LAI and spectral reflectance in the near infrared bands (ETM+ 4). Relatively high correlations are found at the two SWIR bands. The shadow effects could explain the negative correlation at the coniferous forest.

Generally, correlations coefficients are lower at mixed deciduous stands as compared to the coniferous stands. Unlike the plantation coniferous stands, the mixed deciduous stands showed very little variation in the field measured LAI value. The subtle differences in the actual LAI values were thought to be the cause of such relatively low correlation. Among the three datasets, the reflectance from the topographically corrected dataset show higher correlation with the field measured LAI.

Table 1. Correlation coefficients between the field measured LAI and ETM+ reflectance.

Datasets	Forest stands	ETM+1	ETM+2	ETM+3	ETM+4	ETM+5	ETM+7
Raw DN	Combined	0.100	0.031	0.046	-0.364	-0.269	-0.146
	Coniferous	-0.165	-0.255	-0.222	-0.525	-0.556	-0.489
	Deciduous	0.525	0.466	0.461	0.017	0.347	0.396
Atmo-corrected reflectance	Combined	0.156	0.157	0.151	-0.311	-0.001	0.170
	Coniferous	0.094	0.127	0.078	-0.332	-0.034	0.185
	Deciduous	0.359	0.318	0.366	-0.156	0.264	0.312
Topo-corrected reflectance	Combined	0.257	0.166	0.091	-0.437	-0.336	-0.130
	Coniferous	0.193	0.041	-0.084	-0.630	-0.660	-0.241
	Deciduous	0.437	0.426	0.443	-0.055	0.342	0.332

The multiple regression models to predict LAI using five SVIs (NDVI, RSR, BR, GN, WT) were developed by each dataset. To avoid overfitting problem of too many independent variables, we imposed the rule that only three variables can enter for each model. Table 2 shows the selected independent variables, R2 value, and root mean squared error of each of 9 models developed. As noticed from the above correlation coefficients, the R2 values for all combined forest of coniferous and deciduous species is relatively lower as compared to the models for each species group. Although applying two separate models for each species type requires the additional effort of classifying the forest into two groups, it should be a better approach to obtain more reliable LAI map. The RSR, which was developed for the use of both coniferous and deciduous species, did not show any improvement to relate the field measured LAI. We generated the LAI map by applying the two separate models developed by using topographically corrected reflectance data (Fig. 4). Using the forest stand maps, the coniferous and deciduous forests were extracted prior to applying the models.

From the R2 and RMSE value, it is obvious that the topographically corrected reflectance were better to relate with the field measured LAI. The variation of spectral reflectance caused by topographic slope and aspects may exceed the subtle differences from the variation of forest LAI value. Therefore, the radiometric correction of topographic effects should be performed before deriving any meaningful relationship between LAI and spectral reflectance, in particular over the forest on undulated terrain.

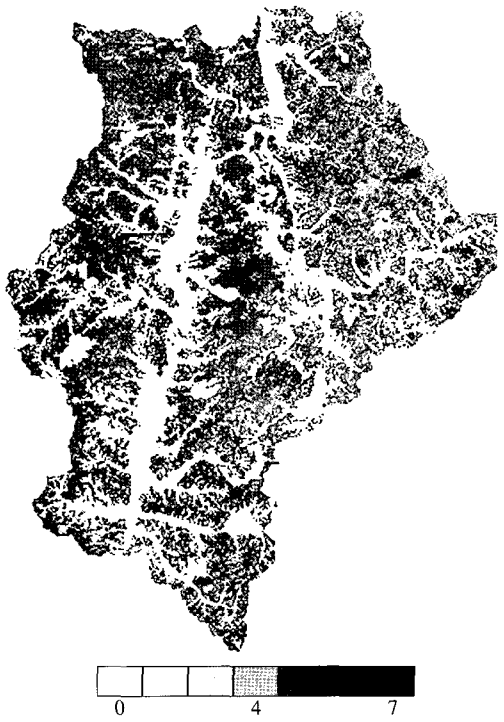

Fig. 4. LAI map generated by applying two separated models for each of coniferous and deciduous forests.

Table 2. Regression models to estimate LAI over the study area.

Datasets	Forest stands	Independent variable selected (SVI)	R^2	RMSE
Raw DN	Combined	NDVI, GN, WT	0.1784	0.8095
	Coniferous	NDVI, BR, GN	0.3895	1.1036
	Deciduous	NDVI, RSR, WT	0.4332	0.4210
Atmo_corrected Reflectance	Combined	NDVI, RSR, GN	0.1574	0.8198
	Coniferous	NDVI, BR, WT	0.2873	1.1924
	Deciduous	NDVI, RSR, GN	0.1604	0.5124
Topo_correted reflectance	Combined	NDVI, GN, WT	0.2660	0.7651
	Coniferous	RSR, BR, GN	0.8018	0.6289
	Deciduous	NDVI, RSR, WT	0.3413	0.4504

5. Conclusions

LAI is an important vegetation structural variable for several applications of quantitative analysis of biophysical process of terrestrial ecosystem. In particular, it can be a crucial parameter related to hydrogical modeling, carbon cycle, climate study at diverse spatial scales. Empirical modeling is quite often an effective way to generate LAI map over large geographic area using satellite remote sensing data.

In an attempt to develop a suitable methodology to generate LAI map over temperate forest in Korea, we tried to relate the field measured LAI value to ETM+ reflectance. When we combined all forest sample plots regardless the species composition, correlation coefficients were relatively low. Significant correlations were found at the plantation coniferous stands. From the modeling approach to link the field measured LAI and the ETM+ spectral reflectance, the major results of this work can be concluded as follows:

- The radiometric correction of topographic effects should be performed on the multispectral remote sensing data that were obtained over the mountainous forest area.
- The sensitivity of spectral reflectance to LAI differs by forest species. Therefore, the empirical model to generate LAI map over the large geographic area should be separately developed for each forest type, rather than using a single model for all forest types.

References

Bonan, G. 1993. Importance of leaf area index and forest type when estimating photosynthesis in boreal forests. *Remote Sensing of Environment*, 43: 303-314.

Badhwar, G.D., R. B. MacDonald, and N. C. Mehta. 1986. Satellite-derived leaf area index and vegetation maps as input to global carbon cycle models - a hierarchical approach. *International Journal of Remote Sensing*, 7(2): 265-281.

Brown, L., J. M. Chen, S. G. Leblanc, and J. Cihlar, 2000. A Shortwave modification to the simple ratio for LAI retrieval in boreal forests: An image and model analysis, *Remote Sensing of Environment*, 71: 16-25.

Carlson, N. T. and D. A. Reley, 1997. On the relation between NDVI, fractional vegetation cover, and leaf area index, *Remote Sensing of Environment*, 62: 241-252.

Chen, J. M. and J. Cihlar, 1996. Retrieving leaf area index of Boreal conifer forests using Landsat TM images, *Remote Sensing of Environment*, 55: 153-162.

Chen, J. M., and S. G. LeBlanc, J. R. Miller, J. Freemantle, S. E. Loechel, C. L. Walthall, K. A. Innanen, and H. P. White, 1999. Compact Airborne Spectrographic Imager (CASI) used for mapping biophysical parameters of boreal forests. *Jour. Of Geophysical Research.* 104 D22: 27945-27958.

Cohen, W. B., T. K. Maierpserger, S. T. Gower, and D. P. Turner, 2003. An improved strategy for regression of biophysical variables and Landsat ETM+ data. *Remote Sensing of Environment*, 84: 561-571.

Crist, E. P., 1985. A TM tasseled cap equivalent transformation for reflectance factor data. *Remote Sensing of Environment*, 17: 301-306.

Curran, P. J., J. Dungan, and H. L. Gholz, 1992. Seasonal LAI measurements in slash pine using Landsat TM. *Remote Sensing of Environment*, 39: 3-13.

Eklundh, L., L. Harrie, and A. Kuusk, 2001, Investigation relationships between Landsat

ETM+ sensor data and leaf area index in a boreal conifer forest, *Remote Sensing of Environment*, 78: 239-251.

Fassnacht, K. S. and T. G. Stith, 1997. Estimating of leaf area index of north central Wisconsin forests using the Landsat Thematic Mapper, *Remote Sensing of Environment*, 61: 229-245.

Gower, S., C. Kucharik, and J. Norman, 1999. Direct and indirect estimation of leaf area index, fAPAR, and net primary production of terrestrial ecosystems. *Remote Sensing of Environment*, 70: 29-51.

Huang, C., B. Wylie, L. Yang, C. Homer and G. Zylstra, 2002. Derivation of a Tasseled Cap Transformation based on Landsat 7 at-satellite reflectance. *International Journal of Remote Sensing*, 23(8): 1741-1748.

Kim, S. H and K. S. Lee, 2003. Local validation of MODIS global Leaf Area Index (LAI) product over temperate forest. *Korean Journal of Remote Sensing*, 19(1): 1-9.

Lee, K. S. and J. S. Yoon, 1997. Radiometric correction of terrain effects for SPOT and Landsat TM imagery in mountainous forest area, *Korean Journal of Remote Sensing*, 13(3): 277-292.

Li-Cor, 1992. *Instruction Manual - LAI2000 Plant Canopy Analyzer*, Li-Cor, Inc. Lincoln, Nebraska, USA.

Nemani, R. R., L. Pierce, S. Running, and L. Band, 1993. Forest ecosystem processes at the watershed scale: Sensitivity to remotely-sensed leaf area index estimates. *International Journal of Remote Sensing*, 14: 2519-2534.

Panferov O., Y. Knyzaikhin, R. B. Myneni, J. Szarzynski, S. Engwald, K. G. Schnitzler, and G. Gravenhorst, 2001. The role of canopy structure in the spectral variation of transmission and absorption of solar radiation in vegetation canopies, *IEEE Transactions on Geoscience and Remote Sensing*, 39(2): 241-253.

Smith, J. A., T. L. Lin, and K. J. Ranson, 1980. The Lambertian assumption and Landsat data, *Photogrammetric Engineering & Remote Sensing*, 46(9): 1183-1189.

Stenberg, P., T. Nilson, H. Smolander, and P. Voipio, 2003. Gap fraction based estimation of LAI in Scots pine stands subjected to experimental removal of branches and stems. *Can. J. Remote Sensing*, 29(3): 363-370.

Tian, Y., Y. Zhang, and Y. Knyazikhin, 2000. Prototyping of MODIS LAI and FPAR algorithm with LASUR and Landsat data, *IEEE Transactions on Geoscience and Remote Sensing*, 38: 2387-2400.

Turner, D., W. Cohen, R. Kennedy, K. Fassnacht, and J. Briggs, 1999. Relationships between leaf area index and Landsat TM spectral vegetation indices across three temperate zone sites. *Remote Sensing of Environment*, 70: 52-68.